Mitogen-activated Protein Kinase Phosphatase-1 Modulates Regional Effects of Injurious Mechanical Ventilation in Rodent Lungs

Moo Suk Park[1,2], Qianbin He[1], Michael G. Edwards[1], Amen Sergew[3], David W. H. Riches[3], Richard K. Albert[1,4], and Ivor S. Douglas[1,4]

[1]Division of Pulmonary Sciences and Critical Care Medicine, University of Colorado Anschutz Medical Campus, School of Medicine, Aurora, Colorado; [2]Division of Pulmonary and Critical Care Medicine, Department of Internal Medicine, Yonsei University College of Medicine, Seoul, Republic of Korea; [3]Program in Cell Biology, Department of Pediatrics, National Jewish Health, Denver, Colorado; and [4]Department of Medicine, Denver Health Medical Center, Denver, Colorado

***Rationale*: Mechanical ventilation induces heterogeneous lung injury by mitogen-activated protein kinase (MAPK) and nuclear factor-κB. Mechanisms regulating regional injury and protective effects of prone positioning are unclear.**

***Objectives*: To determine the key regulators of the lung regional protective effects of prone positioning in rodent lungs exposed to injurious ventilation.**

***Methods*: Adult rats were ventilated with high (18 ml/kg, positive end-expiratory pressure [PEEP] 0) or low V_T (6 ml/kg; PEEP 3 cm H_2O; 3 h) in supine or prone position. Dorsal–caudal lung mRNA was analyzed by microarray and MAPK phosphatases (MKP)-1 quantitative polymerase chain reaction. MKP-$1^{-/-}$ or wild-type mice were ventilated with very high (24 ml/kg; PEEP 0) or low V_T (6–7 ml/kg; PEEP 3 cm H_2O). The MKP-1 regulator PG490-88 (MRx-108; 0.75 mg/kg) or phosphate-buffered saline was administered preventilation. Injury was assessed by lung mechanics, bronchioalveolar lavage cell counts, protein content, and lung injury scoring. Immunoblotting for MKP-1, and IκBα and cytokine ELISAs were performed on lung lysates.**

***Measurements and Main Results*: Prone positioning was protective against injurious ventilation in rats. Expression profiling demonstrated MKP-1 20-fold higher in rats ventilated prone rather than supine and regional reduction in p38 and c-jun N-terminal kinase activation. MKP-$1^{-/-}$ mice experienced amplified injury. PG490-88 improved static lung compliance and injury scores, reduced bronchioalveolar lavage cell counts and cytokine levels, and induced MKP-1 and IκBα.**

***Conclusions*: Injurious ventilation induces MAPK in an MKP-1–dependent fashion. Prone positioning is protective and induces MKP-1. PG490-88 induced MKP-1 and was protective against high V_T in a nuclear factor-κB–dependent manner. MKP-1 is a potential target for modulating regional effects of injurious ventilation.**

AT A GLANCE COMMENTARY

Scientific Knowledge on the Subject

Injurious mechanical ventilation amplifies acute lung injury in a heterogeneous and regional fashion but the molecular mechanisms underlying regional lung injury and the protective effects of prone positioning are unclear.

What This Study Adds to the Field

Regionally injurious ventilation is associated with discrete differential lung transcriptomic changes. Ventilating in the prone compared with the supine position abrogates regional injury by depressing mitogen-activated protein kinase phosphatases-1, and mitogen-activated protein kinase phosphatases-1 deficiency amplifies injurious ventilation. Pretreatment with the antiinflammatory PG490-88 (MRx-108, a triptolide-derivative) is protective by reducing mitogen-activated protein kinase and nuclear factor-κB–dependent lung cytokine expression in ventilator-induced lung injury.

Keywords: regionally injurious ventilation; prone position; rodent lung injury; MKP-1/DUSP-1; triptolide

Mechanical ventilation with high V_T can cause ventilator-induced lung injury (VILI), which can amplify acute lung injury (ALI) and increase the mortality of acute respiratory distress syndrome (1). Ventilation-associated lung injury has been attributed to mechanical damage of tissues and cells because of overdistention (volutrauma) or cyclical airspace opening and closing (atelectrauma) resulting in the production, release, or activation of cytotoxic and inflammatory cascades (biotrauma) (2–6).

Injurious ventilation in the supine position (SPV) is generally characterized by lung injury that is spatially heterogeneous (7) with a greater atelectasis and consolidation in dorsal–caudal regions. This heterogeneity is less pronounced after ventilation in the prone position (PPV) (8–11) and PPV may be lung protective in ALI and acute respiratory distress syndrome (12). PPV increases dorsal–caudal end-inspiratory lung volumes, improves ventilation–perfusion matching, and alters chest-wall mechanics reducing regionally heterogeneous changes in ventilation (9). Whether molecular mechanisms are involved in regulating regional differences between PPV and SPV has not been previously assessed.

The intracellular mitogen-activated protein kinase (MAPK) and nuclear factor-κB (NF-κB) signaling pathways are key regulators of inflammation in the development of VILI (13–15). Therefore, strategies to modulate MAPK activation may have therapeutic benefit. The MAPK pathways are tonically regulated

(*Received in original form September 3, 2011; accepted in final form April 17, 2012*)

Supported by NIH P30HL101295 and HL068628.

Author Contributions: Conception, hypotheses delineation, design, analysis and interpretation of data, writing, and acquisition of the data, M.S.P., I.S.D., and R.K.A.; acquisition of the data and writing, A.S., D.W.H.R., and Q.H.; and analysis of data, M.G.E.

This study was presented in part at the 2011 American Thoracic Society annual international conference.

Correspondence and requests for reprints should be addressed to Ivor S. Douglas, M.D., Division of Pulmonary and Critical Care Medicine, Denver Health and University of Colorado, Department of Medicine, MC 4000, 777 Bannock Street, Denver, CO 80204. E-mail: idouglas@dhha.org

This article has an online supplement, which is accessible from this issue's table of contents at www.atsjournals.org

Am J Respir Crit Care Med Vol 186, Iss. 1, pp 72–81, Jul 1, 2012

Originally Published in Press as DOI: 10.1164/rccm.201109-1593OC on May 10, 2012
Internet address: www.atsjournals.org

by negative feedback from MAPK phosphatases (MKP) and dual specificity phosphatases (DUSP). MKP-1/DUSP-1 is the protypical regulator of p38 MAPK (p38) and c-jun N-terminal kinase (JNK) (16–18). The regional effects of PPV on these signal pathways have not been previously assessed.

We hypothesized that the stresses and strains that are produced by injurious ventilation and lead to VILI occur on a regional basis, and that PPV is protective against VILI through regional dampening of the molecular pathways that regulate the responses to these stresses and strains. To determine the key regulators of the lung regional protective effects of PPV in rodent lungs exposed to injurious ventilation, we assessed changes in gene expression in a rat model of VILI and found evidence indicating that MKP-1 regulated the inflammatory signaling pathways. We confirmed the central role of MKP-1 in a murine model of injurious ventilation using MKP-1 knock-out (MKP-$1^{-/-}$) mice. In addition, we characterized the effects of pretreatment with the MKP-1 regulator, PG490-88, on injurious ventilation and MKP-1 expression.

METHODS

Animals and *In Vivo* VILI Models

Experiments were conducted in accordance with protocols approved by the University of Colorado Institutional Animal Care and Use Committee. Complete details are in the online supplement.

Rats. Male Harlan Sprague-Dawley rats (340–400 g; Indianapolis, IN) were anesthetized and a tracheotomy and jugular cannulation performed before random allocation to one of two ventilation strategies: low VT (LVT; 6 ml/kg actual body weight; respiratory rate [RR], 70–80/ min; positive end-expiratory pressure [PEEP], 3 cm H_2O) or high VT (HVT; 18 ml/kg; RR, 40 breaths/min; PEEP, 0 cm H_2O), in either the prone or supine position (PPV or SPV, respectively) for up to 3 hours. Nonventilated rats were used as control animals.

Mice. MKP-$1^{-/-}$ mice (Bristol-Myers Squibb, Sunnyvale, CA) (19) on a C57BL6/129-mixed background were bred and typed (*see* Table E1 and Figure E1 in the online supplement) from cryopreserved embryos (Dr. Yusen Liu, Columbus, OH) (20). C57B6/129 (wild-type [WT], Jackson Laboratories, Bar Harbor, ME) were used as control animals.

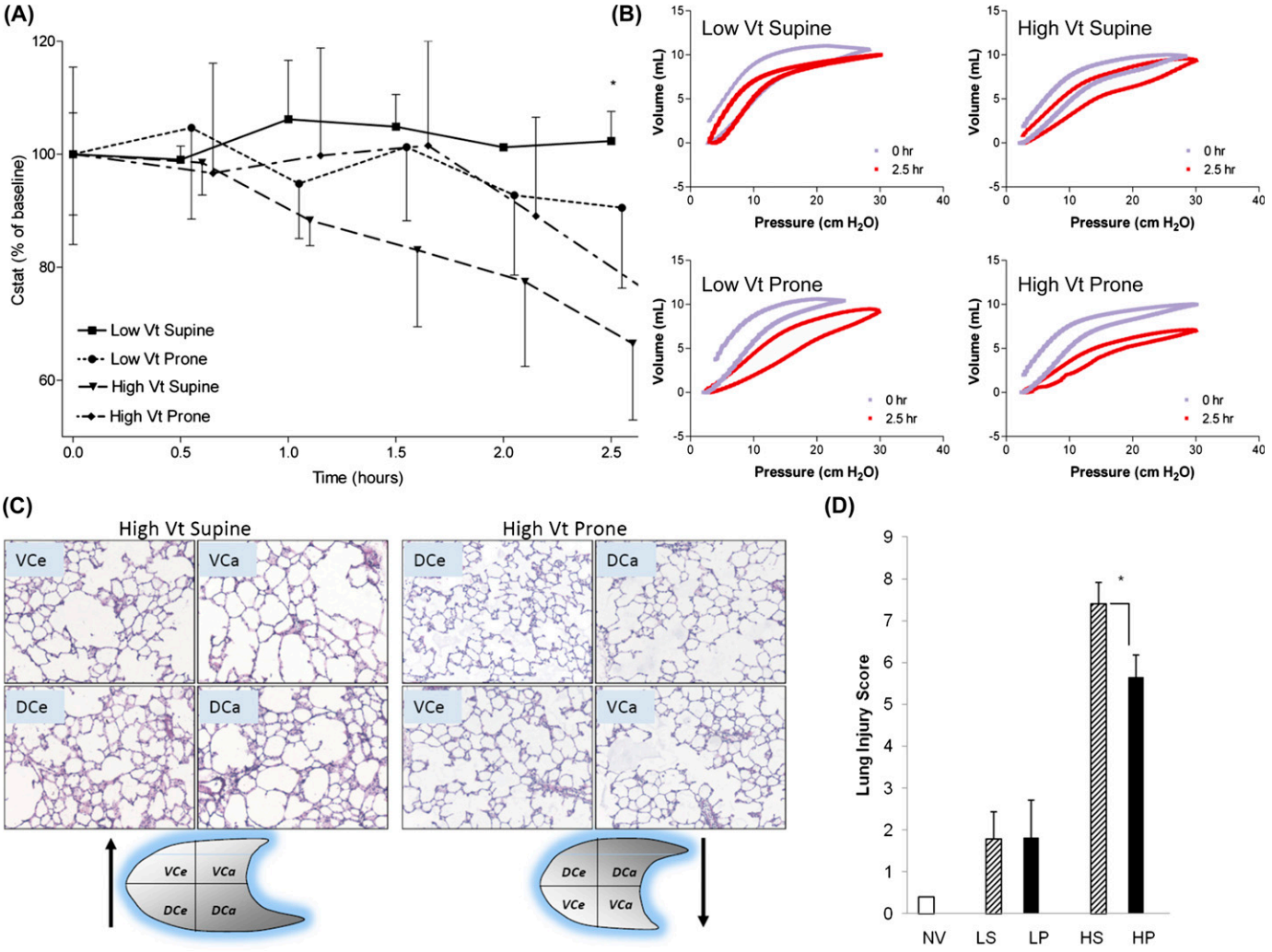

Figure 1. Injurious effects of high VT ventilation and modulating lung regional effects of ventilation in the prone position in rats. Sprague-Dawley rats (340–400 g; Indianapolis, IN) were ventilated for up to 3 hours with low VT (6 ml/kg; respiratory rate, 70–80/m; positive end-expiratory pressure, 3 cm H_2O) or high VT (18 ml/kg; respiratory rate, 40 breaths/min; positive end-expiratory pressure, 0 cm H_2O). Additionally, animals were ventilated in prone (P) or supine (S) position (n = 3 per condition). Lung mechanics were measured every 30 minutes. (*A*) Percent change of static respiratory system compliance (Cstat) over time from baseline, RMANOVA * $P < 0.05$. (*B*) Quasistatic pressure–volume curve illustrating lung compliance change from baseline (0 h, *blue line*) to 2.5 hours (*red line*) for the four ventilation groups. (*C*) Hematoxylin and eosin sections of each lung quadrant (VCe = ventral–cephalad, VCa = ventral–caudal, DCe = dorsal–cephalad, DCa = dorsal–caudal) after high VT ventilation in supine (*left*) and prone (*right*) position. (*D*) Semiquantitative lung injury scoring of DCa quadrant after ventilation. HP = high VT prone; HS = high VT supine; LP = low VT prone; LS = low VT supine; NV = nonventilated. *$P < 0.05$.

Male mice (6–8 wk) were ventilated with either very high VT (VHVT; 24 ml/kg; RR, 100 breaths/min; PEEP, 0 cm H_2O) or LVT (6–7 ml/kg; RR, 150 breaths/min; PEEP, 3 cm H_2O) ventilation for 2–3 hours in the supine position. PG490-88 (MRx-108; 0.75 mg/kg generously provided by MyeloRx LLC, Vallejo, CA) (21) or phosphate buffered saline (PBS) was injected intraperitoneally in mice 30 minutes before beginning either VHVT or LVT mechanical ventilation.

On completion of the ventilation protocols, animals were killed and lung tissue was harvested for analysis.

Histopathology

Inflation-fixed lungs were paraffin-embedded; divided into four regions (dorsal–cranial, dorsal–caudal, ventral–cranial, and ventral–caudal); and sectioned in 5-μm slices. Semiquantitative grading of lung injury on hematoxylin and eosin sections was as previously described (*see* online supplement) (22).

RNA Extraction and Microarray Methods

RNA was isolated from dorsal–caudal lung quadrants (n = 3 per condition; RNeasy kits; Qiagen Inc., Valencia, CA), and prepared using standard protocols for hybridization to 230 2.0 Affymetrix microarrays (Santa Clara, CA).

Informatics and Pathway Analyses

Microarray data were analyzed and visualized using Partek Genomics Suite v 6.5 (Partek, St. Louis, MO). Biologic themes differentially affected by PPV versus SPV injurious ventilation were identified using a modified Fisher's exact test (Ingenuity Pathway Analysis; http://www.ingenuity.com).

Quantitative Real-Time Polymerase Chain Reaction

Real-time polymerase chain reaction for MKP-1 was performed using cDNA transcribed from whole-lung mRNA (iCycler; Biorad, Inc., Hercules, CA) using reagent kits and primers (*see* online supplement). β-actin was the housekeeping control.

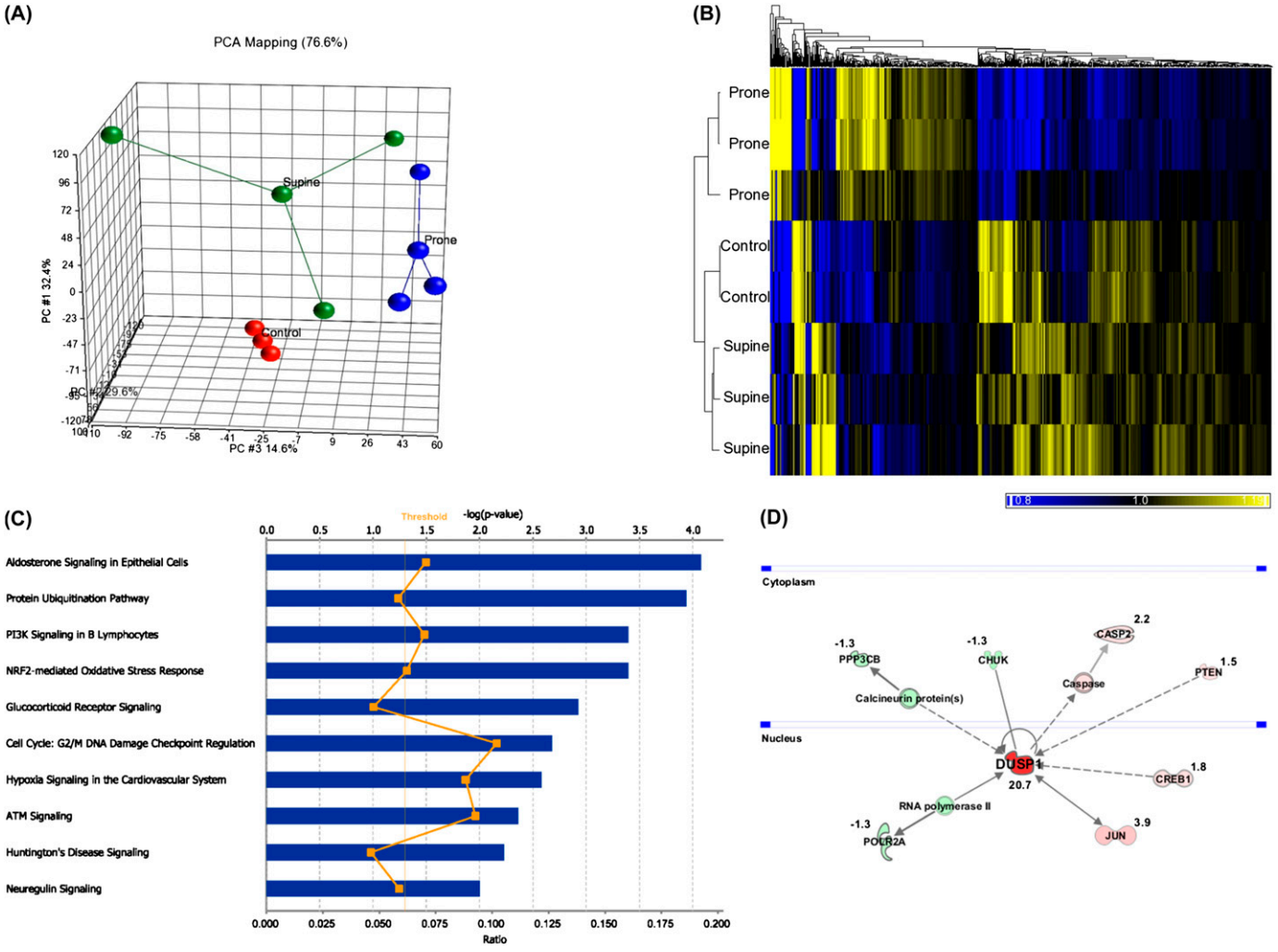

Figure 2. Differential whole-lung mRNA expression in rats dorsal–caudal lung quadrants after high VT ventilation. mRNA from whole lung was subjected to microarray and resultant differential gene expression levels were analyzed using bioinformatic approaches. (*A*) Multidimensional scaling plot. In the principal components analysis (PCA), each experimental sample is represented as a solid shape for which the position in space is determined by genome-wide transcript levels. The centroid estimate for sample clusters represents mean multidimensional expression for each experimental condition. *Red* = nonventilated control, *Green* = supine, *Blue* = prone. (*B*) Hierarchical clustering analysis heatmap generated by Euclidean distance dissimilarity matrix and average linkage for genes differentially expressed between ventilation in the supine position, prone, and nonventilated lungs. Genes colored *yellow* represent an increase above the mean for the gene; genes in *blue* represent a decrease from the mean; and genes in *black* approximate the mean expression across all samples. (*C*) Significantly overrepresented biologic themes (pathways) differentially affected by prone (P) versus supine (S) injurious ventilation. −log *P* for each theme indicated in top axis. (*D*) Interactome of dual specificity phosphatases (DUSP)-1/mitogen-activated protein kinase phosphatase-1 (most significantly [20.7-fold] over expressed in P versus S; $P < 0.003$) indicating the major site of action (cytoplasomc or nuclear) of their products. Genes in *green* are expressed at a relatively lower level in P versus S and genes in *red* at a higher level.

TABLE 1. TEN MOST DIFFERENTIALLY UP-REGULATED AND 10 MOST DIFFERENTIALLY DOWN-REGULATED GENES (OF 705) BETWEEN PRONE AND SUPINE HIGH V_T LUNGS BASED ON AVERAGE CHANGE IN EXPRESSION (FOLD CHANGE)

		Mean Log_2 Expression			Prone versus Supine		
Affy ID	Symbol	Nonventilated	Prone	Supine	Fold Δ	*P* Value	Gene Name
1387282_at	Hspb8	5.4	9.9	5.1	27.3	1.69×10^{-2}	heat shock protein B8
1368147_at	Dusp1	7.9	8.5	4.1	20.7	2.76×10^{-2}	dual specificity phosphatase 1
1395572_at	Dnaja4	5	9.1	5.2	14.9	4.59×10^{-2}	DnaJ (Hsp40) homolog, subfamily A, member 4
1369584_at	Socs3	3.6	7.6	3.8	14.4	4.68×10^{-3}	suppressor of cytokine signaling 3
1385620_at	Hsph1	7.5	13.8	10.2	12.1	7.31×10^{-3}	heat shock 105 kDa/110 kDa protein 1
1386935_at	Nr4a1	9	12.1	8.8	10.2	1.13×10^{-2}	nuclear receptor subfamily 4, group A, member 1
1368290_at	Cyr61	10	11	7.7	9.7	7.02×10^{-3}	cysteine-rich, angiogenic inducer, 61
1369583_at	Jdp2	6.3	8	4.9	8.5	2.94×10^{-2}	Jun dimerization protein 2
1383302_at	Dnajb1	8.2	12.6	9.6	8	7.76×10^{-3}	DnaJ (Hsp40) homolog, subfamily B, member 1
1394970_at	Cars	3.1	6.6	3.8	6.7	3.43×10^{-2}	cysteinyl-tRNA synthetase
1395848_at	LOC683962	6.1	5.1	7.1	−4	1.96×10^{-2}	similar to NIPA-like domain containing 3
1390139_a_at	Obsl1	6.7	4.6	6.6	−4	2.24×10^{-2}	obscurin-like 1
1384377_at	Ddx28	6.6	4.2	6.3	−4	3.27×10^{-2}	DEAD (Asp-Glu-Ala-Asp) box polypeptide 28
1382066_at	R3hdm2	4.9	4.7	6.8	−4.3	4.03×10^{-2}	R3H domain containing 2
1381221_at	RGD1311300	7.3	4.5	6.7	−4.4	2.48×10^{-2}	similar to T cell receptor V delta 6
1369412_a_at	Slc19a1	4.7	4	6.1	−4.4	4.45×10^{-2}	solute carrier family 19 (folate transporter), member 1
1370382_at	RT1-Db1	7.3	6.9	9.2	−4.8	3.22×10^{-2}	RT1 class II, locus Db1
1390931_at	Adamts15	10	8.2	10.6	−5.3	1.13×10^{-2}	ADAM metallopeptidase with thrombospondin type 1 motif, 15
1370499_at	Klrb1a	8.6	4.8	7.7	−7.5	4.16×10^{-2}	killer cell lectin-like receptor subfamily B, member 1A
1368505_at	Rgs4	8.1	5.7	9.8	−18.1	2.75×10^{-2}	regulator of G-protein signaling 4

Cytokine ELISA

Murine-specific immunoreactive keratinocyte-derived chemokine (KC), macrophage inflammatory protein-2 (MIP-2), and IL-6 concentrations in whole-lung lysates were quantified using ELISA kits (ElisaTech, Aurora, CO).

Western Blot Analysis

Sodium dodecyl sulfate–polyacrylamide gel electrophoresis and immunoblotting were performed using whole-lung homogenates essentially as previously described (22).

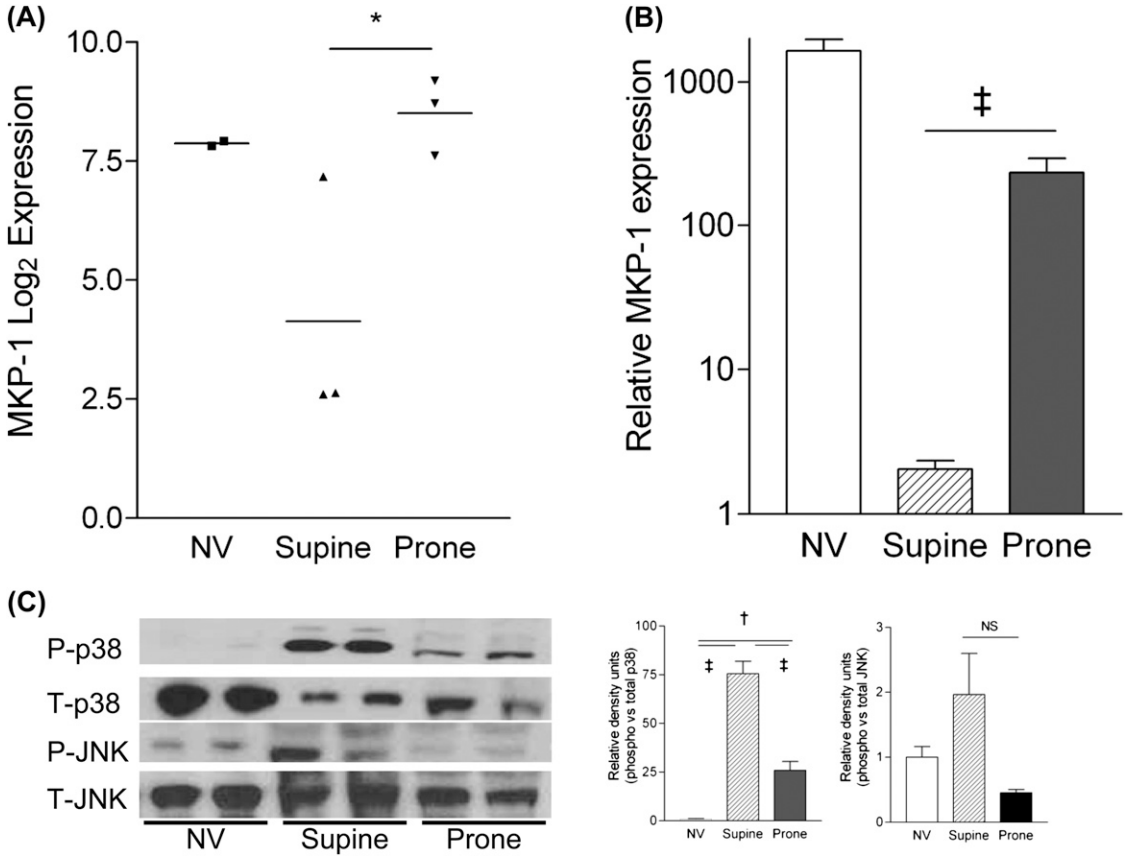

Figure 3. Mitogen-activated protein kinase phosphatase (MKP)-1 mRNA expression in dorsal–caudal rat lung segments after injurious ventilation. (*A*) Dot-plot of MKP-1/dual specificity phosphatases mRNA expression (Log_2) in the microarray analyses. Bar indicates mean of expression for each condition. (*B*) Relative β-actin normalized, MKP-1 mRNA expression by quantitative polymerase chain reaction (mean ± SD) in the same lung samples as *A*. (*C*) Western blotting of mitogen-activated protein kinase expression (p38 and JNK) with relative densitometry (mean ± SD) of phospho-to-total protein expression. JNK = c-jun N-terminal kinase; NS = significant; NV = nonventilated; P = phosphor; T = total. $^*P < 0.05$, $^\dagger P < 0.01$, $^\ddagger P < 0.001$.

Lung Tissue Immunohistochemistry

Immunohistochemical stains were performed applying a standard avidin-biotin complex technique on paraffin-embedded lung.

Statistical Analysis for Physiologic and Signaling Studies

Data are presented as means ± SD for each group. Prism v3.11 (GraphPad, La Jolla, CA) was used for one-way and repeated-measures analysis of variance (ANOVA) or paired *t* tests with *post hoc* analyses (Bonferroni/Dunn) for comparison of multiple groups. *P* less than 0.05 was considered significant.

RESULTS

Prone Position Mitigates the Effects of Injurious Ventilation

After 2.5 hours of ventilation, static respiratory system compliance (Cstat) fell more in animals receiving HVT than those receiving LVT (mean ± SD change, −32.9 ± 10.8% vs. −4.75 ± 10.1%; $P = 0.05$) (Figure 1A). Similar changes were seen in pressure–volume (PV)-loop hysteresis (Figure 1B). No differences were observed with respect to the change in Cstat in animals ventilated supine versus prone.

Lung injury was more severe in animals ventilated with HVT compared with LVT, regardless of body position, and was more severe in animals receiving HVT in the supine compared with the prone position (Figures 1C and 1D). In dependent and nondependent segments, lung injury was more severe in lung segments from supine ventilated rats than comparable zones from prone ventilated rats (*see* Figure E2). Furthermore, lung injury was less in dorsal–caudal (nondependent) lung quadrant of rats ventilated prone than in the dorsal–caudal (dependent) quadrant in rats ventilated supine (mean [± SD] lung injury score in dorsal–caudal quadrants after HVT, supine 7.4 ± 0.52 vs. prone 5.65 ± 0.53; $P < 0.05$) (Figures 1C and 1D).

Discrete Transcriptomes Differentiate Prone from Supine Dorsal–Caudal Lung after HVT

We observed large and consistent differential lung regional gene transcriptional effects of positioning and injurious ventilation (Figure 2). A statistically defined set of 705 differentially expressed transcripts was identified in arrays from lungs of animals receiving HVT ventilation when prone versus supine ($P < 0.05$) (*see* Figure E3). A consistent pattern of gene expression change was appreciated in principal components analysis (Figure 2A) and in the cluster analysis dendrogram (Figure 2B). The lung expression in nonventilated animals and in those ventilated prone clustered with narrow confidence boundaries, whereas clustering in those ventilated supine was discrete in multidimensional space but with more variation. Discrete global expression patterns separated lungs from animals ventilated supine or prone (median [interquartile range] percent coefficient of variation supine 7.36%, [3.98–13.58%] vs. prone 5.63% [2.84–11.06%]; *F* test $P < 0.00001$).

The 10 highest and lowest differentially expressed genes based on average fold change in expression are presented in Table 1 (*see* Table E2 for a complete gene list). Biologic themes underlying these expression patterns were identified based on the overrepresentation of predefined groups of transcripts within the statistically defined set. The most overrepresented pathways are presented in Figure 2C (*see* Table E2 for complete pathway list). Among these, DUSP-1/MKP-1 was an interacting molecule in five discrete pathways (Figure 2D; *see* Table E2) and DUSP-1/MKP-1 mRNA expression was increased 20-fold in lungs of animals ventilated prone versus supine ($P = 0.0276$) (Figure 3A) suggesting that MKP-1 was an important and significantly overrepresented transcript associated with the effect of PPV on regionally injurious ventilation in dorsal–caudal lung.

Prone Position Regulates Expression of MKP-1 and MAPKs

To confirm the more than 20-fold differential expression in lungs from animals ventilated prone versus supine we measured the MKP-1 mRNA expression in dorsal–caudal rat lung (Figure 3B). Consistent with the microarray expression pattern (Figure 3A) MKP-1 expression from HVT animals ventilated supine was down-regulated compared with lungs from nonventilated animals. PPV was associated with significantly less down-regulation than SPV or nonventilated lungs (ANOVA, $P < 0.0001$). Additionally, MKP-1 expression was relatively higher in ventral cephalad and ventral caudal but not dorsal cephalad lung quadrants from prone ventilated rats versus those ventilated supine (*see* Figure E4).

To determine the functional effects of position-related regional MKP-1 expression changes we measured activity of the major MAPK inflammatory signaling pathway proteins. The levels of phosphorylated p38 were increased in the dorsal–caudal segments of lungs from animals ventilated supine compared with that from lungs of animals that were not ventilated or those ventilated prone. (Figure 3C) (p-p38, $P < 0.05$; p-JNK, $P =$ NS). pERK (p44/42) expression was induced to a comparable level in HVT prone and HVT supine lungs compared with nonventilated controls (data not shown).

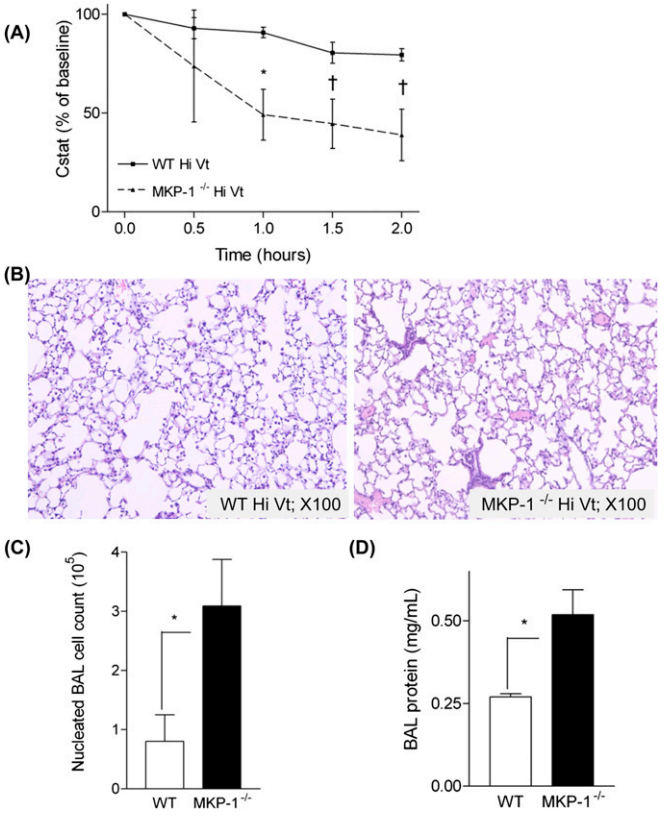

Figure 4. Injurious effects of high VT ventilation in mitogen-activated protein kinase phosphatase (MKP)-1$^{-/-}$ mice. (*A*) Time course comparison of static lung compliance (Cstat) % changes (mean at each time point ± SD) from baseline between wild-type (WT) and MKP-1$^{-/-}$ mice during high VT ventilation. (*B*) Lung hematoxylin and eosin histology in WT and MKP-1$^{-/-}$ mice after 2 hours of high VT ventilation demonstrating increased vascular engorgement, alveolar wall edema, and cellular infiltration. (*C*) Total bronchoalveolar lavage (BAL) cell count (mean ± SD). (*D*) BAL protein concentration (mean ± SD). *$P < 0.05$, †$P < 0.01$.

Mice Deficient in MKP-1 (MKP-1$^{-/-}$) Are More Susceptible to VILI

To investigate the role of MKP-1 in VILI, we evaluated the effect of VHVT in MKP-1$^{-/-}$ and WT mice (n = 4 each). Decreases in Cstat were greater in MKP-1$^{-/-}$ than WT mice after VHVT ventilation (mean ± SD % change, MKP-1$^{-/-}$ −20.6 ± 3.1%, WT −6.17 ± 13%; $P < 0.01$) (Figure 4A).

Histologic evidence of lung injury was comparable between WT and MKP-1$^{-/-}$ mice (Figure 4B, lung injury scores not shown) but bronchoalveolar lavage cell counts and protein concentrations were greater in WT than in MKP-1$^{-/-}$ mice (WT 0.9 ± 0.52 × 10^5 vs. MKP-1$^{-/-}$ 1.57 ± 0.9 × 10^5 cells/ml; $P < 0.05$ Figure 4C, and protein 0.27 ± 0.02 vs. 0.52 ± 0.15 μg/ml, $P < 0.05$ Figure 4D, respectively).

PG490-88 Pretreatment Is Protective against VILI

Cstat % changes at 2 hours from baseline were significantly higher in animals receiving PBS plus HVt ventilation than PBS plus LVT or those receiving PG490-88 and either HVT or LVT ($P < 0.001$) (Figure 5A). These changes were reflected in pressure–volume (PV) loop hysteresis (Figure 5B).

Cell counts in the bronchoalveolar lavage fluid were lower in the PBS plus LVT, PG490-88 plus HVT, and LVT than in the PBS plus HVT group ($P < 0.001$) (Figure 5C).

Compared with animals that were not ventilated, whole-lung MIP-2 and KC were increased in lungs of animals receiving PBS plus HVT ($P < 0.001$) and PG490-88 plus HVT ($P < 0.001$; n = 3 for each). Levels were also increased, but less so, in the LVT groups (n = 3 for each). IL-6 levels were similar in the four groups but MIP-2 and KC levels trended lower in the PG490-88 plus HVT and PG490-88 plus LVT groups than in the PBS plus HVT group (Figure 5D). Lung injury was less in PG490-88 plus HVT and PG490-88 plus LVT groups compared with PBS plus HVT lungs (Figures 6A–6D) ($P < 0.05$).

PG490-88 Induces Lung MKP-1 and IkBα Expression in VILI

Consistent with the response to HVT ventilation in rats, whole-lung MKP-1 expression from mice was 50% lower in lungs ventilated with VHVT than with HVT (Figure 7A). PG490-88

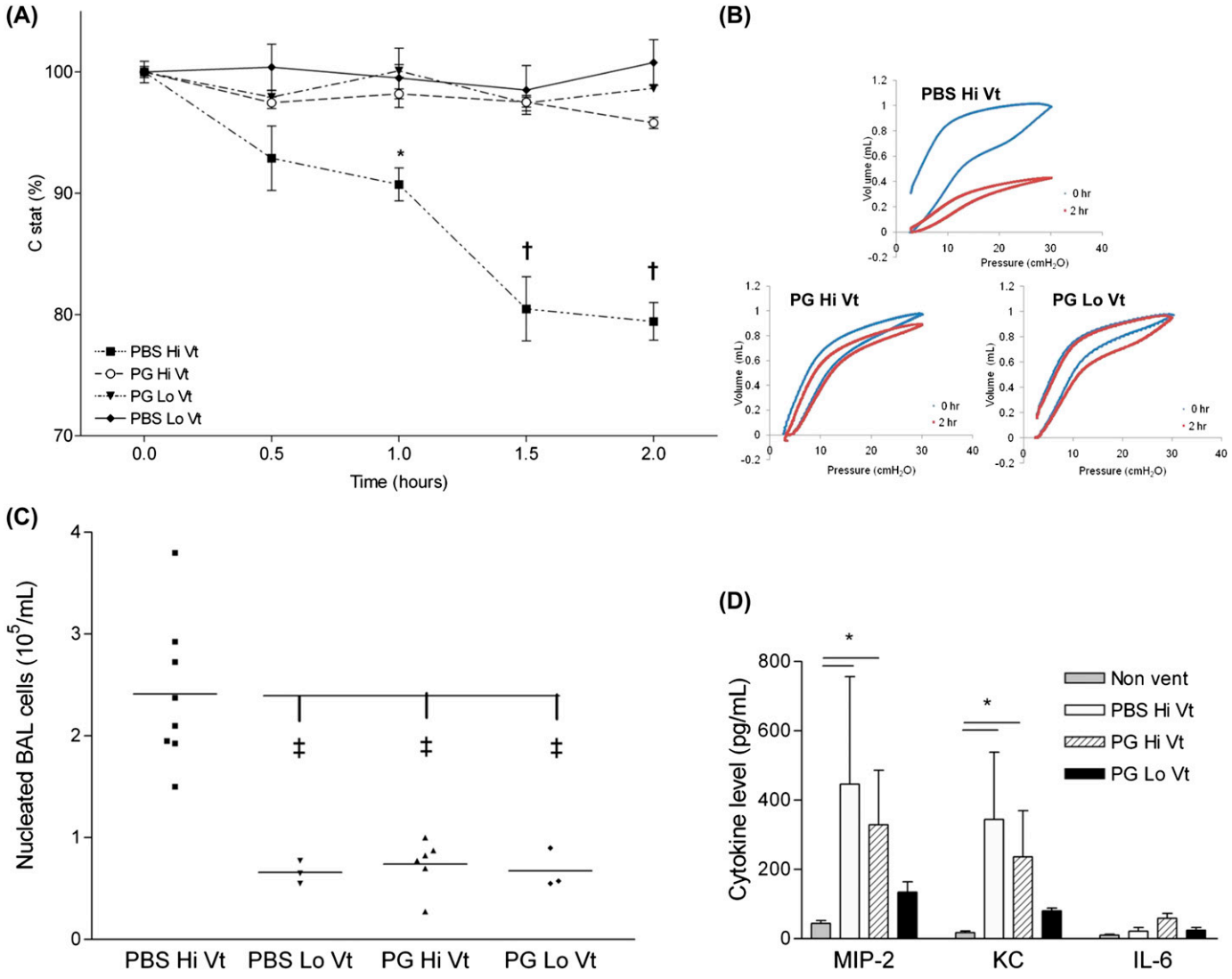

Figure 5. Effect of PG490-88 (PG) pretreatment on the progression and magnitude of injurious ventilation in mice. Mice were ventilated with high VT (HVT, 24 ml/kg) or low VT (LVT, 7 ml/kg) 30 minutes after intraperitoneal 0.75 mg/kg PG or phosphate-buffered saline (PBS). (*A*) Static lung compliance (Cstat) % change from baseline (mean at each time point ± SD). (*B*) Quasistatic pressure–volume curves illustrating lung compliance change from baseline (0 h; *blue line*) to 2 hours (*red line*) for the three groups. (*C*) Dot plot of bronchoalveolar lavage (BAL) total cell counts in PBS-HVT and LVT, PG HVT, and LVT groups (bar is mean for each group). (*D*) Whole-lung lysates cytokine levels (MIP-2, KC, and IL-6) in nonventilated (non vent) control, PBS-High VT, and PG-High and PG-Low VT groups (mean ± SD). *$P < 0.05$, †$P < 0.01$, ‡$P < 0.001$. KC = keratinocyte-derived chemokine; MIP = macrophage inflammatory protein.

pretreatment induced higher MKP-1 expression than PBS in mice subjected to HVT but expression was lower than in PG490-88 plus LVT. Immunostainable MKP-1 was detectable in alveolar corner cells and bronchial epithelial cells in lungs after PG490-88 despite HVT ventilation (Figures 7B and 7C). HVT induced modest pERK and pP38 activation compared with LVT but PG490-88 pretreatment did not significantly block ERK or p38 activation (*see* Figure E5). However, IκBα expression was increased in PG490-88 plus HVT compared with PBS plus HVT animals (*see* Figure E5) suggesting potential downstream involvement of NF-κB–dependent pathways in the protective effect of PG490-88 pretreatment before injurious ventilation.

DISCUSSION

We have shown that HVT ventilation preferentially affects dependent lung zones relative to nondependent regions; is reduced by prone positioning; is regulated by MKP-1 and NF-κB–dependent pathways; and that a triptolide derivative, PG490-88, induces MKP-1 and protects against VILI through NF-κB.

Our microarray studies of lungs from rats ventilated prone with HVT demonstrated regional overexpression of MAPK-related genes relative to expression of when the animals were ventilated supine. Injurious mechanical ventilation induces differential expression of a large number of transcripts in the lung many of which are involved in immunity, inflammation, apoptosis (23) development, cellular communication, and the cytoskeleton (24). The mechanosensing and transduction mechanisms by which the physical forces associated with injurious ventilation initiate intracellular signals include matrix-cytoskeleton interactions (25) and stretch activated ion channels (26) among others. However, effective pharmacotherapy targeting these mechanisms has yet to emerge.

Previous gene expression studies in VILI were potentially confounded by averaging global lung gene expression and disregarding regional effects of injurious ventilation (24, 27, 28). The novel aspect of the present study is the substantial regional differential gene expression in response to injurious ventilation, particularly in the MAPK pathway, measured in dorsal–caudal lung segments in varying body position.

The three major MAPKs as p38, ERK, and JNK have previously been implicated in lung injury and the inflammatory response to injurious ventilation (13, 14, 29, 30). We previously reported specific TLR-4/ERK-MAPK dependent inflammation in a LPS lipid-A ALI model (22). Injurious ventilation, by contrast, is associated with an early increase in p-p38 and pERK (13). Our findings replicate those of Damarla and coworkers (29) who demonstrated p38 phosphorylation after 4 hours of injurious ventilation. However, there are conflicting data regarding JNK phosphoactivation, perhaps related to the VT used for ventilation. Abdulnour and colleagues (13) reported no significant JNK-activation in murine lungs after 120 minutes of ventilation with VT of 20 ml/kg. By contrast, Li and coworkers (30) found significant JNK activation after 60 minutes of ventilation with VT of 30 ml/kg.

Our rat microarray study elucidated lung regional down-regulation of MKP-1/DUSP-1 expression in dorsal–caudal lung segments from animals receiving injurious SPV and significantly less down-regulation in dorsal–caudal lung after PPV. This effect of PPV on MKP-1 expression was also apparent in ventral–cephalad and dorsal–cephalad lung segments but not ventral–caudal lung segments, possibly as a result of attenuated lung regional protective effects of PPV against injurious ventilation in that segment.

MKP-1 can act as a biologic damper on the MAPK pathway by dephosphorylating p-p38 and pJNK MAP kinases (31, 32). MKP-1 is induced by a number of antiinflammatory drugs (33) suggesting the possibility that pharmacotherapy could limit VILI.

MAPK signaling has been implicated in stretch-induced epithelial barrier dysfunction (34) and host immunity (35). The finding that somatic MKP-$1^{-/-}$ amplified the injurious effects of HVT ventilation is consistent with previous reports showing that MKP-$1^{-/-}$ mice are hyperresponsive to low-dose LPS toxicity (36) and to gram-positive cell wall proteins, peptidoglycan, or lipoteichoic acid (37) with resulting sustained activation of p38 and c-JNK and derepression of serum proinflammatory cytokine levels, resulting in increased mortality from septic shock (20, 37). Consistent with our findings, Qian and coworkers (38) demonstrated that MKP-5– (DUSP10) deficient mice developed significantly more severe ALI in response to intratracheal LPS in association with enhanced MAPK phosphorylation and macrophage-derived proinflammatory cytokine production.

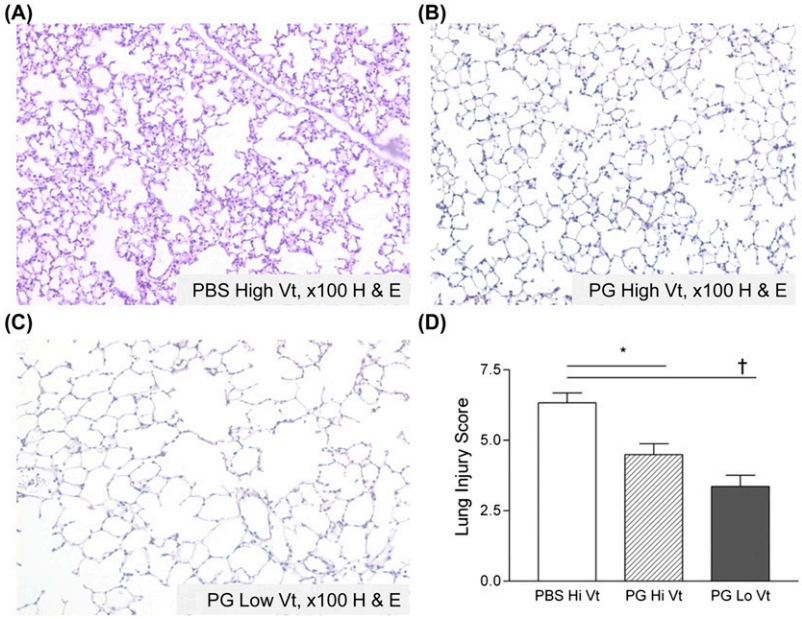

Figure 6. Effect of PG490-88 (PG) on murine lung injury after high and low VT ventilation. Representative sections from mice after ventilation (*A*) PBS + HVT, (*B*) PG + HVT, (*C*) PG + LVT. (*D*) Semiquantitative lung injury scores (mean ± SD) $^{*}P < 0.05$, $^{\dagger}P < 0.01$. H&E = hematoxylin and eosin; PBS = phosphate-buffered saline.

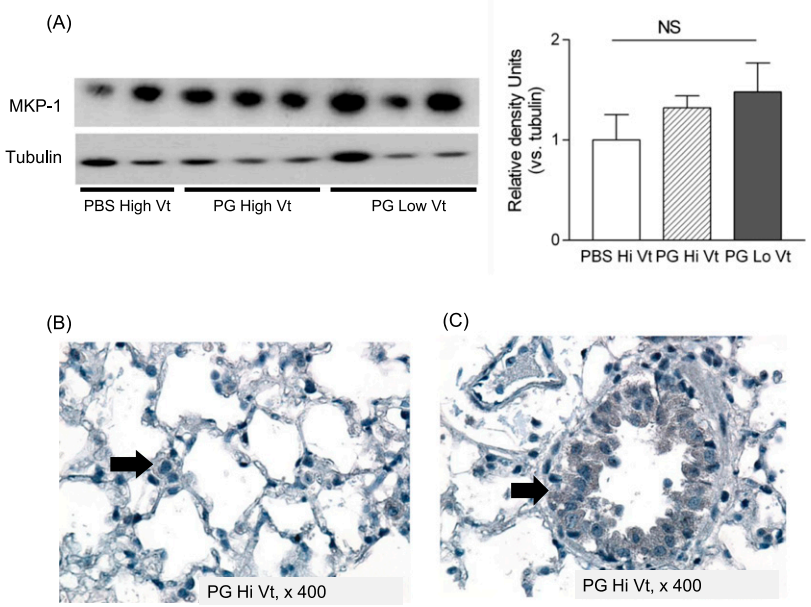

Figure 7. Effect of PG490-88 (PG) on lung mitogen-activated protein kinase phosphatase (MKP)-1 expression in wild-type mice after high (24 ml/kg) or low (7 ml/kg) V_T ventilation. (*A*) Western blotting of whole-lung lysates for MKP-1 with tubulin control from phosphate-buffered saline (PBS) + HV_T, PG + HV_T, and PG + LV_T mice. Semiquantative densitometry (mean ± SD) demonstrates nonsignificant (NS) increase in MKP-1 expression in PG-treated mice. (*B*) Immunohistochemical staining of MKP-1 in alveolar corner cells. (*C*) Immunohistochemical staining of MKP-1 in bronchial epithelial cells.

Our observations were limited to global MKP-1–dependent effects of injurious ventilation. Whether MKP-1 deficiency regulates lung regional barrier integrity, surfactant biosynthesis, and inflammation are focus areas of continued investigation.

Triptolide, a diterpene triepoxide from *Tripterygium wilfordii* (Thunder-god vine), inhibits agonist-induced IL-6 and IL-8 expression in human bronchial epithelial cells i*n vivo* (39) and chlorine gas–induced lung injury *in vivo* (40) and has been used to treat cancer, inflammatory and autoimmune diseases, and organ transplantation rejection. PG490-88 is a 14-succinyl water-soluble prodrug of PG490 triptolide sodium, is a putative immunoregulator, and prevents bleomycin-induced lung fibrosis (21).

Triptolide is purported to be an effective inhibitor of agonist-induced MKP-1 expression but the mechanisms of triptolide's antiinflammatory and antitumor mechanism are controversial (21, 41–43). The magnitude and persistence of the regulatory effects on MKP-1 expression may be temporal, cell, and context-specific. Triptolide suppresses LPS-induced expression of MKP-1 in RAW264.7 (33) and MH-S alveolar macrophages lines and primary alveolar macrophages (44) *in vitro* resulting in derepression of ERK1/2, p38, and JNK MAPK. Notably, triptolide was only an effective inhibitor of LPS-induced MKP-1 expression in doses higher than 0.5 μM (33, 45). Koo and coworkers (41) reported that triptolide inhibited growth of immortalized HT22 hippocampal cells by suppression of MKP-1 expression resulting in persistent ERK1/2 activation. Inexplicably, however, despite significantly reduced MKP-1 expression in triptolide-treated cells, p-JNK and p-p38 expression was unchanged compared with control (41). This inconsistency is further highlighted by data from Koo and coworkers (41) who demonstrated that triptolide-pretreatment blocked dexamethasone- and LPS-induced MKP-1 expression, thus enhancing p-JNK and p-p38 expression in cultured microglial cells.

Consistent with protective effects reported in bleomycin (21) and chlorine gas–induced lung injury (40), PG490-88 was highly protective against VILI and was associated with a modest increase in total lung MKP-1 expression even at the dose of 0.75 mg/kg we selected to minimize toxicity.

Because mechanical stimuli mediate the release of inflammatory cytokines by increasing phosphorylation of the cytoplasmic-sequestering protein IκBα and nuclear translocation of NF-κB (15), we considered the possibility that PG490-88 may also have an inhibitory effect on NF-κB–mediated inflammation (46–48) and VILI (15).

Belperio and coworkers (49) reported that injurious ventilation induced IκBα phosphorylation, enhanced CXC chemokine expression, and caused VILI. Chiang and coworkers (1) demonstrated that anti–NF-κB antibodies were effective at preventing lung edema and inflammation in an isolated perfused VILI model. Consistent with these data, our study demonstrated that PG490-88 abrogated VILI in mice in association with IκBα stabilization resulting in reduced lung expression of proinflammatory CXC-2 chemokines, MIP-2, and KC.

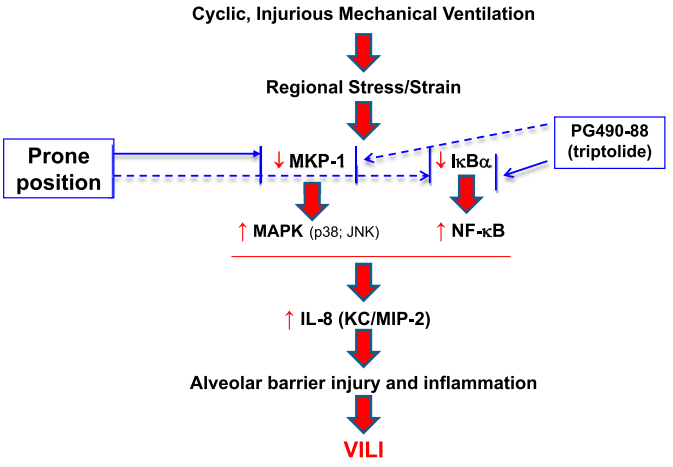

Figure 8. Model of injurious mechanical ventilatory effects on mitogen-activated protein kinase phosphatase (MKP)-1, mitogen-activated protein kinase (MAPK), and nuclear factor (NF)-κB signaling in the lung. Cyclic injurious ventilation amplifies regional lung cytokine expression, alveolar barrier injury, and inflammation progressing to ventilator-induced lung injury (VILI) through suppression of MKP-1, activation of NF-κB, p38, and JNK. Prone position reduces MAPK-dependent signaling by inducing MKP-1 and possibly IκB kinase. PG490-88 (triptolide) induces MKP-1 and IkB expression and blocks VILI and lung cytokine release. JNK = c-jun N-terminal kinase; KC = keratinocyte-derived chemokine; MIP = macrophage inflammatory protein.

This study has several limitations. First, our studies may have overestimated the effects of PPV on VILI. Because of technical limitations, we measured respiratory system compliance as a crude indicator of global VILI in VHVT ventilated rat. Regional lung imaging, transpulmonary pressure measurements with functional partitioning of lung mechanics, and parallel blood gas assessments could potentially have informed the analyses.

Second, the VT used in VHVT ventilation was unphysiologic and imposed on previously healthy, noninjured rodents. Accordingly, an intermediate VT may have resulted in less pronounced effects. However, our gene expression data indicating that effects of injurious ventilation are regionally heterogeneous underline the notion that a safe threshold for "lung-protective" VT has not yet been identified. It is also possible that if imposed as a "second-hit" after the onset of pneumonia or pulmonary contusion, the lung regional effects of injurious ventilation and body position may have differed. Furthermore, the relevance of these observations in human ALI is also unknown. Third, the effects of injurious ventilation in MKP-1 deletion mice are likely to be more complex than those we have described and are the focus of continued study. Lastly, we used a preinjury treatment model to assess the effects of PG490-88. Studies to determine the effects of PG490-88 after induction of VILI will be important in further characterizing the inflammation-regulating effects of this compound. Our study adds to the accumulating evidence derived from advanced imaging technologies (6) and high-throughput "omics" approaches (50) indicating that that even VTs considered to be "lung protective" have the potential to be injurious even in the absence of a priming pulmonary insult (51).

In conclusion, injurious ventilation increased MAPK activation and inflammatory cytokine expression through decreased MKP-1 (*see* Figure E2) and enhanced NF-κB activation. Prone positioning is regionally protective with increased expression of MKP-1 in dorsal–caudal lung and associated reductions in p38 and JNK activation. PG490-88 is globally protective and abrogates propagation of VILI in association with inhibition of NF-κB–dependent MAPK signaling and possibly by MKP-1 regulation (Figure 8). MKP-1 is an important potential target for modulating lung regional effects of injurious ventilation.

Author disclosures are available with the text of this article at www.atsjournals.org.

Acknowledgment: The authors thank John M. Fidler, Ph.D. (MyeloRx, LLC) for generously providing MRx108 (PG490-88) for these studies. They also acknowledge Mario Perez, B.Sc., Benjamin Edelman, B.Sc., Eric Schmidt, M.D., and Yimu Yang, M.D., for technical assistance and Rubin Tuder, M.D., for assistance with data interpretation and manuscript review.

REFERENCES

1. Chiang CH, Pai HI, Liu SL. Ventilator-induced lung injury (VILI) promotes ischemia/reperfusion lung injury (I/R) and NF-kappaB antibody attenuates both injuries. *Resuscitation* 2008;79:147–154.
2. Pinhu L, Whitehead T, Evans T, Griffiths M. Ventilator-associated lung injury. *Lancet* 2003;361:332–340.
3. Crosby LM, Waters CM. Epithelial repair mechanisms in the lung. *Am J Physiol Lung Cell Mol Physiol* 2010;298:L715–L731.
4. Plotz FB, Slutsky AS, van Vught AJ, Heijnen CJ. Ventilator-induced lung injury and multiple system organ failure: a critical review of facts and hypotheses. *Intensive Care Med* 2004;30:1865–1872.
5. Vlahakis NE, Schroeder MA, Limper AH, Hubmayr RD. Stretch induces cytokine release by alveolar epithelial cells in vitro. *Am J Physiol* 1999;277:L167–L173.
6. Bellani G, Guerra L, Musch G, Zanella A, Patroniti N, Mauri T, Messa C, Pesenti A. Lung regional metabolic activity and gas volume changes induced by tidal ventilation in patients with acute lung injury. *Am J Respir Crit Care Med* 2011;183:1193–1199.
7. Ricard JD, Dreyfuss D, Saumon G. Production of inflammatory cytokines in ventilator-induced lung injury: a reappraisal. *Am J Respir Crit Care Med* 2001;163:1176–1180.
8. Altemeier WA, McKinney S, Krueger M, Glenny RW. Effect of posture on regional gas exchange in pigs. *J Appl Physiol* 2004;97:2104–2111.
9. Broccard A, Shapiro RS, Schmitz LL, Adams AB, Nahum A, Marini JJ. Prone positioning attenuates and redistributes ventilator-induced lung injury in dogs. *Crit Care Med* 2000;28:295–303.
10. Broccard AF, Shapiro RS, Schmitz LL, Ravenscraft SA, Marini JJ. Influence of prone position on the extent and distribution of lung injury in a high tidal volume oleic acid model of acute respiratory distress syndrome. *Crit Care Med* 1997;25:16–27.
11. Santana MC, Garcia CS, Xisto DG, Nagato LK, Lassance RM, Prota LF, Ornellas FM, Capelozzi VL, Morales MM, Zin WA, *et al*. Prone position prevents regional alveolar hyperinflation and mechanical stress and strain in mild experimental acute lung injury. *Respir Physiol Neurobiol* 2009;167:181–188.
12. Gattinoni L, Carlesso E, Taccone P, Polli F, Guerin C, Mancebo J. Prone positioning improves survival in severe ARDS: a pathophysiologic review and individual patient meta-analysis. *Minerva Anestesiol* 2010; 76:448–454.
13. Abdulnour RE, Peng X, Finigan JH, Han EJ, Hasan EJ, Birukov KG, Reddy SP, Watkins JE III, Kayyali US, Garcia JG, *et al*. Mechanical stress activates xanthine oxidoreductase through MAP kinase-dependent pathways. *Am J Physiol Lung Cell Mol Physiol* 2006;291:L345–L353.
14. Dolinay T, Wu W, Kaminski N, Ifedigbo E, Kaynar AM, Szilasi M, Watkins SC, Ryter SW, Hoetzel A, Choi AM. Mitogen-activated protein kinases regulate susceptibility to ventilator-induced lung injury. *PLoS One* 2008;3:e1601.
15. Held HD, Boettcher S, Hamann L, Uhlig S. Ventilation-induced chemokine and cytokine release is associated with activation of nuclear factor-kappaB and is blocked by steroids. *Am J Respir Crit Care Med* 2001;163:711–716.
16. Clark AR, Martins JR, Tchen CR. Role of dual specificity phosphatases in biological responses to glucocorticoids. *J Biol Chem* 2008;283: 25765–25769.
17. King EM, Holden NS, Gong W, Rider CF, Newton R. Inhibition of NF-kappaB-dependent transcription by MKP-1: transcriptional repression by glucocorticoids occurring via p38 MAPK. *J Biol Chem* 2009;284:26803–26815.
18. Li L, Chen SF, Liu Y. MAP kinase phosphatase-1, a critical negative regulator of the innate immune response. *Int J Clin Exp Med* 2009;2: 48–67.
19. Dorfman K, Carrasco D, Gruda M, Ryan C, Lira SA, Bravo R. Disruption of the ERP/MKP-1 gene does not affect mouse development: normal MAP kinase activity in ERP/MKP-1-deficient fibroblasts. *Oncogene* 1996;13:925–931.
20. Zhao Q, Wang X, Nelin LD, Yao Y, Matta R, Manson ME, Baliga RS, Meng X, Smith CV, Bauer JA, *et al*. MAP kinase phosphatase 1 controls innate immune responses and suppresses endotoxic shock. *J Exp Med* 2006;203:131–140.
21. Krishna G, Liu K, Shigemitsu H, Gao M, Raffin TA, Rosen GD. PG490-88, a derivative of triptolide, blocks bleomycin-induced lung fibrosis. *Am J Pathol* 2001;158:997–1004.
22. Fang WF, Cho JH, He Q, Lin MC, Wu CC, Voelkel NF, Douglas IS. Lipid a fraction of LPS induces a discrete MAPK activation in acute lung injury. *Am J Physiol Lung Cell Mol Physiol* 2007;293:L336–L344.
23. Nonas SA, Moreno-Vinasco L, Ma SF, Jacobson JR, Desai AA, Dudek SM, Flores C, Hassoun PM, Sam L, Ye SQ, *et al*. Use of consomic rats for genomic insights into ventilator-associated lung injury. *Am J Physiol Lung Cell Mol Physiol* 2007;293:L292–L302.
24. Dolinay T, Kaminski N, Felgendreher M, Kim HP, Reynolds P, Watkins SC, Karp D, Uhlig S, Choi AM. Gene expression profiling of target genes in ventilator-induced lung injury. *Physiol Genomics* 2006;26: 68–75.
25. Taniguchi LU, Caldini EG, Velasco IT, Negri EM. Cytoskeleton and mechanotransduction in the pathophysiology of ventilator-induced lung injury. *J Bras Pneumol* 2010;36:363–371.
26. Hamanaka K, Jian MY, Weber DS, Alvarez DF, Townsley MI, Al-Mehdi AB, King JA, Liedtke W, Parker JC. TRPV4 initiates the acute calcium-dependent permeability increase during ventilator-induced lung injury in isolated mouse lungs. *Am J Physiol Lung Cell Mol Physiol* 2007;293: L923–L932.
27. dos Santos CC, Okutani D, Hu P, Han B, Crimi E, He X, Keshavjee S, Greenwood C, Slutsky AS, Zhang H, *et al*. Differential gene profiling

in acute lung injury identifies injury-specific gene expression. *Crit Care Med* 2008;36:855–865.
28. Nonas SA, Finigan JH, Gao L, Garcia JG. Functional genomic insights into acute lung injury: role of ventilators and mechanical stress. *Proc Am Thorac Soc* 2005;2:188–194.
29. Damarla M, Hasan E, Boueiz A, Le A, Pae HH, Montouchet C, Kolb T, Simms T, Myers A, Kayyali US, *et al*. Mitogen activated protein kinase activated protein kinase 2 regulates actin polymerization and vascular leak in ventilator associated lung injury. *PLoS ONE* 2009;4: e4600.
30. Li LF, Yu L, Quinn DA. Ventilation-induced neutrophil infiltration depends on c-jun N-terminal kinase. *Am J Respir Crit Care Med* 2004; 169:518–524.
31. Camps M, Nichols A, Arkinstall S. Dual specificity phosphatases: a gene family for control of map kinase function. *FASEB J* 2000;14:6–16.
32. Keyse SM. Protein phosphatases and the regulation of mitogen-activated protein kinase signalling. *Curr Opin Cell Biol* 2000;12:186–192.
33. Chen P, Li J, Barnes J, Kokkonen GC, Lee JC, Liu Y. Restraint of proinflammatory cytokine biosynthesis by mitogen-activated protein kinase phosphatase-1 in lipopolysaccharide-stimulated macrophages. *J Immunol* 2002;169:6408–6416.
34. Oudin S, Pugin J. Role of map kinase activation in interleukin-8 production by human beas-2b bronchial epithelial cells submitted to cyclic stretch. *Am J Respir Cell Mol Biol* 2002;27:107–114.
35. Chi H, Barry SP, Roth RJ, Wu JJ, Jones EA, Bennett AM, Flavell RA. Dynamic regulation of pro- and anti-inflammatory cytokines by MAPK phosphatase 1 (MKP-1) in innate immune responses. *Proc Natl Acad Sci USA* 2006;103:2274–2279.
36. Salojin KV, Owusu IB, Millerchip KA, Potter M, Platt KA, Oravecz T. Essential role of MAPK phosphatase-1 in the negative control of innate immune responses. *J Immunol* 2006;176:1899–1907.
37. Wang X, Meng X, Kuhlman JR, Nelin LD, Nicol KK, English BK, Liu Y. Knockout of MKP-1 enhances the host inflammatory responses to gram-positive bacteria. *J Immunol* 2007;178:5312–5320.
38. Qian F, Deng J, Gantner BN, Flavell RA, Dong C, Christman JW, Ye RD. MAP kinase phosphatase 5 protects against sepsis-induced acute lung injury. *Am J Physiol Lung Cell Mol Physiol* 2012;302:L866–L874.
39. Zhao G, Vaszar LT, Qiu D, Shi L, Kao PN. Anti-inflammatory effects of triptolide in human bronchial epithelial cells. *Am J Physiol Lung Cell Mol Physiol* 2000;279:L958–L966.
40. Hoyle GW, Hoyle CI, Chen J, Chang W, Williams RW, Rando RJ. Identification of triptolide, a natural diterpenoid compound, as an inhibitor of lung inflammation. *Am J Physiol Lung Cell Mol Physiol* 2010;298:L830–L836.
41. Koo HS, Kang SD, Lee JH, Kim NH, Chung HT, Pae HO. Triptolide inhibits the proliferation of immortalized ht22 hippocampal cells via persistent activation of extracellular signal-regulated kinase-1/2 by down-regulating mitogen-activated protein kinase phosphatase-1 expression. *J Korean Neurosurg Soc* 2009;46:389–396.
42. Tai CJ, Wu AT, Chiou JF, Jan HJ, Wei HJ, Hsu CH, Lin CT, Chiu WT, Wu CW, Lee HM, *et al*. The investigation of mitogen-activated protein kinase phosphatase-1 as a potential pharmacological target in non-small cell lung carcinomas, assisted by non-invasive molecular imaging. *BMC Cancer* 2010;10:95.
43. Geng Y, Fang M, Wang J, Yu H, Hu Z, Yew DT, Chen W. Triptolide down-regulates COX-2 expression and PGE2 release by suppressing the activity of NF-kappaB and MAP kinases in lipopolysaccharide-treated pc12 cells. *Phytother Res* 2012;26:337–343.
44. Zhao Q, Shepherd EG, Manson ME, Nelin LD, Sorokin A, Liu Y. The role of mitogen-activated protein kinase phosphatase-1 in the response of alveolar macrophages to lipopolysaccharide: attenuation of proinflammatory cytokine biosynthesis via feedback control of p38. *J Biol Chem* 2005;280:8101–8108.
45. Hu J-H, Chen T, Zhuang Z-H, Kong L, Yu M-C, Liu Y, Zang J-W, Ge B-X. Feedback control of MKP-1 expression by p38. *Cell Signal* 2007; 19:393–400.
46. Jung YJ, Isaacs JS, Lee S, Trepel J, Neckers L. IL-1beta-mediated up-regulation of HIF-1alpha via an NF-kappaB/COX-2 pathway identifies HIF-1 as a critical link between inflammation and oncogenesis. *FASEB J* 2003;17:2115–2117.
47. Uhlig U, Fehrenbach H, Lachmann RA, Goldmann T, Lachmann B, Vollmer E, Uhlig S. Phosphoinositide 3-OH kinase inhibition prevents ventilation-induced lung cell activation. *Am J Respir Crit Care Med* 2004;169:201–208.
48. Yang Y, Liu Z, Tolosa E, Yang J, Li L. Triptolide induces apoptotic death of T lymphocyte. *Immunopharmacology* 1998;40:139–149.
49. Belperio JA, Keane MP, Burdick MD, Londhe V, Xue YY, Li K, Phillips RJ, Strieter RM. Critical role for CXCR2 and CXCR2 ligands during the pathogenesis of ventilator-induced lung injury. *J Clin Invest* 2002;110:1703–1716.
50. Ma SF, Grigoryev DN, Taylor AD, Nonas S, Sammani S, Ye SQ, Garcia JG. Bioinformatic identification of novel early stress response genes in rodent models of lung injury. *Am J Physiol Lung Cell Mol Physiol* 2005;289:L468–L477.
51. Wolthuis EK, Vlaar AP, Choi G, Roelofs JJ, Juffermans NP, Schultz MJ. Mechanical ventilation using non-injurious ventilation settings causes lung injury in the absence of pre-existing lung injury in healthy mice. *Crit Care* 2009;13:R1.